
# Supplemental Material

# Unlocking GOES: A Statistical Framework for Quantifying the Evolution of Convective Structure in Tropical Cyclones Supplemental Materials

Trey McNeely, Ann B. Lee, Kimberly M. Wood, Dorit Hammerling

## ORB Statistics

Here we present some supplemental details on the computation of the thresholded ORB functions. Full details on thresholded ORB features can be found in McNeely et al. (2019).

**Global Organization: Defining $\psi(T, \mathbf{s})$.** Global Organization is based on deviation angles (Pineros et al., 2008). We begin with the image gradient, $\nabla T(\mathbf{s})$, which is obtained by applying a Sobel filter to a smoothed (via a 50-km gaussian blur) image of $T(x, y)$. Then, at any point $\mathbf{s}$, consider a circle centered on the TC with radius $|\mathbf{s}|$, and let $\mathbf{v}(\mathbf{s})$ be a (counter-clockwise) tangent vector at that point. Then, define an intermediate angle, $\phi(T, \mathbf{s})$, to be the angle representing the shortest rotation from $\mathbf{v}(\mathbf{s})$ to $\nabla T(\mathbf{s})$. That is,

$$\phi(T, \mathbf{s}) = \angle\Big(\mathbf{v}(\mathbf{s}), \nabla T(\mathbf{s})\Big), \tag{1}$$

where the angle $\phi$ in $[0, \pi]$ takes its largest value $\pi$ when $\nabla T(\mathbf{s}) \parallel -\mathbf{v}(\mathbf{s})$ and takes its smallest value of 0 when $\nabla T(\mathbf{s}) \parallel \mathbf{v}(\mathbf{s})$. When the gradient either points towards or away from the image center, $\phi$ takes values near $\pi/2$.

We then define the deviation angle $\psi$ in $[-\pi/2, \pi/2]$ as a quantity which takes values 0 when $\nabla T(\mathbf{s})$ points along the line between the TC center and $\mathbf{s}$, and that has its maximum magnitude when $\nabla T(\mathbf{s})$ is perpendicular to that line. Formally,

$$\psi(T, \mathbf{s}) = \phi(T, \mathbf{s}) - \pi/2 = \angle\Big(\mathbf{v}(\mathbf{s}), \nabla T(\mathbf{s})\Big) - \pi/2. \tag{2}$$

Then, small magnitudes of $\psi$ indicate adherence to axisymmetric organization, and large magnitudes (near $\pm\pi/2$) indicate extreme deviations from that idealized vortex.

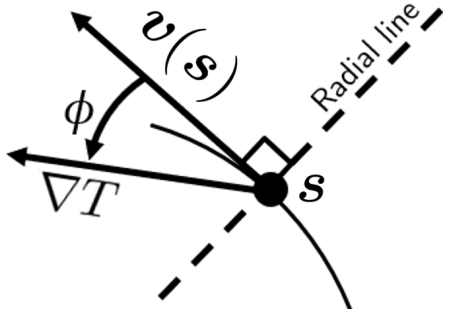


Figure 1: *Visualizing deviation angles:* The deviation angle at a given point $\mathbf{s}$ is based on the direction of the image gradient ($\nabla T(\mathbf{s})$) at $\mathbf{s}$ relative to a counter-clockwise tangent vector $\mathbf{v}(\mathbf{s})$ to an origin-centered circle through $\mathbf{s}$. In the figure above, the deviation angle $\psi = \phi - \pi/2$, where $\psi$ is the shortest angle between $\nabla T(\mathbf{s})$ and $\mathbf{v}(\mathbf{s})$. $\psi = 0$ when the gradient is aligned with the radial line in either direction, and $\psi = \pm\pi/2$ when $\nabla T(\mathbf{s}) = \mp\mathbf{v}(\mathbf{s})$, respectively.

**Radial Structure: Centering.** The primary complication in computing $\overline{T}(T;r)$ comes from defining the location of $r = 0$. In order to *automate image centering*, we generate radial profiles for many image centers, then defining the center of the image as the center resulting in a maximum average value of $T(\mathbf{s})$ over the eye of the storm. The eye is defined here as

$$\mathcal{E} = \{\mathbf{s} \mid 0 < |\mathbf{s}| < \underset{0<r<100\text{km}}{\arg\min}\ \overline{T}(r)\}. \tag{3}$$

In words, $\mathcal{E}$ comprises the radii less than the radius of global minimum average temperature. In practice, we also check that $\overline{T}(T;0) \geq \min_r \overline{T}(r) + \kappa$, where $\kappa$ determines a minimum depth of the eye (difference between eye and eyewall temperatures; 25°C in our implementation); if this condition is not met, we consider there to be no clearly IR-visible eye at this center, and, if no IR-visible eye is found at any candidate center, we revert to the best-track center. When an eye-eyewall structure is visible in $\text{CTT}_b$, this clarifies it in $\overline{T}(r)$. This eye-based center is also passed to the computation of $\texttt{DAV}(r)$ when it differs from the best-track center. The definition for the eye $\mathcal{E}$ was originally part of this suite of features. We no longer treat summaries of $\mathcal{E}$ as features; it is merely retained for this centering process.

**Bulk Morphology: Sector Ratios.** In addition to `SIZE` and `SKEW` of $\mathcal{L}(T;c)$, a skew-agnostic asymmetry measure is obtained from the smoothed radial integration of $\mathcal{L}(T;c)$ given by

$$\rho(\theta, T; c) = \frac{\int_{S_\theta \bigcap \mathcal{L}(T;c)} dA}{\int_{\mathcal{L}(T;c)} dA}, \tag{4}$$

where $S_\theta = \left\{(r,\phi) :\ r \leq r_{max},\ \theta - \frac{\delta\theta}{2} \leq \phi \leq \theta + \frac{\delta\theta}{2}\right\}$ and $dA$ is the area element for polar coordinates. In words, $\rho(\theta, T; c)$ denotes the fraction of $\mathcal{L}(T;c)$ which lies within $\frac{\delta\theta}{2}$ of $\theta$. We take $\delta\theta = \frac{\pi}{6}$. `SHAPE` and `ECC` both measure how circular $\rho(\theta, T; c)$ is, providing insight into raggedness [`SHAPE`; mean absolute deviation of $\rho(\theta, T; c)$ from its median value] and stretching [`ECC`; the eccentricity of an ellipse with major and minor axes defined by the radii of circles bounding and bounded by $\rho(\theta, T; c)$] of $\mathcal{L}(T;c)$, respectively.

# References


McNeely, T., A. B. Lee, D. Hammerling, and K. Wood, 2019: Quantifying the spatial structure of tropical cyclone imagery. NCAR tech note. Tech. rep., NCAR Technical Note NCAR/TN-557+STR. doi:10.5065/5frb-ws04.

Pineros, M. F., E. A. Ritchie, and J. S. Tyo, 2008: Objective measures of tropical cyclone structure and intensity change from remotely sensed infrared image data. *IEEE Transactions on Geoscience and Remote Sensing*, **46 (11)**, 3574–3580.

# Visualizing Functional ORB Features

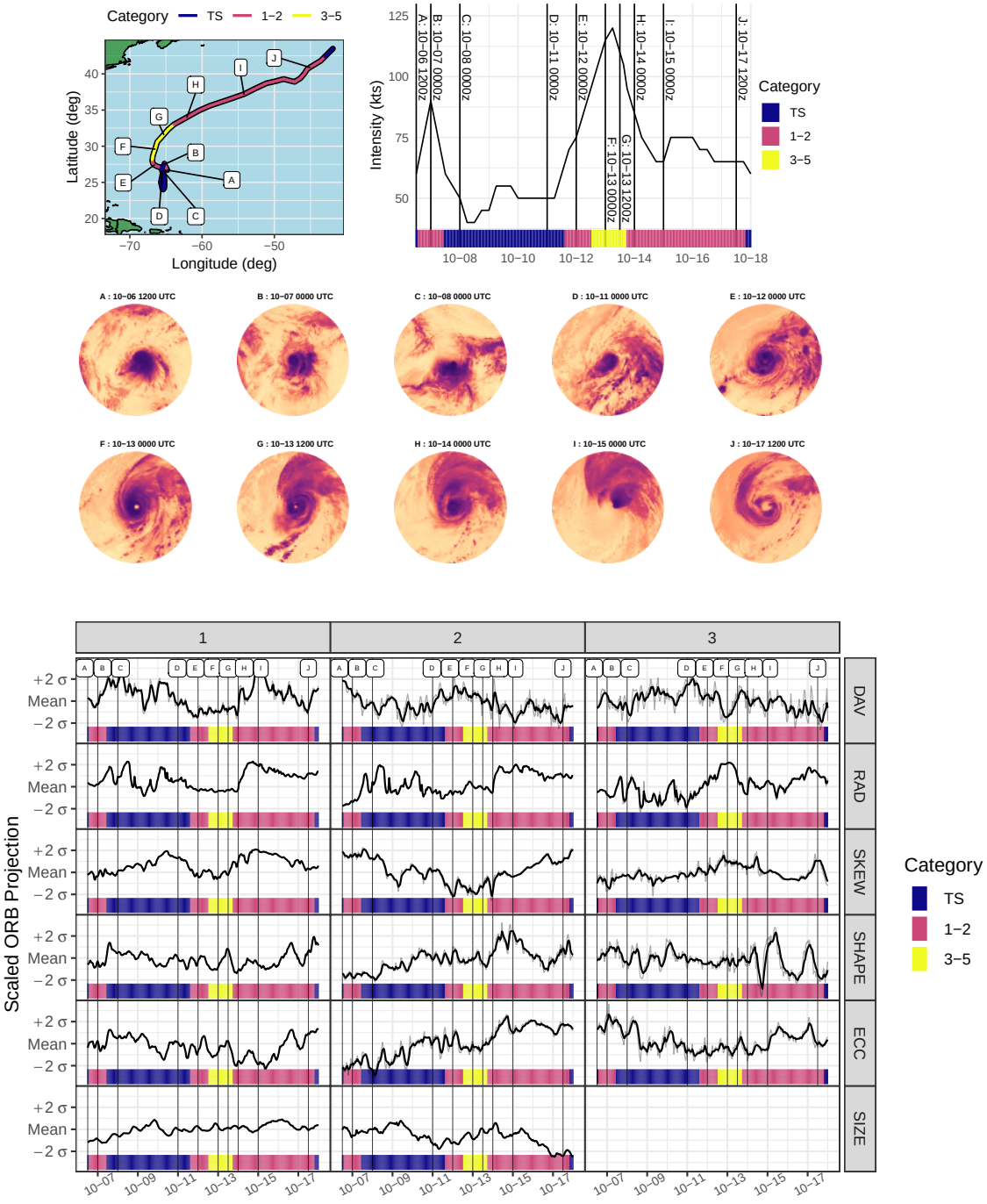


Figure 2: *Full ORB evolution of Nicole [2016] with selected stamps:* A map shows the trajectory of Nicole (top-left) with select points (A-J) labeled. The intensity over time is shown with the same points labeled (top-right), showing the two intensification and weakening cycles. GOES imagery is shown for the 10 labeled points (center), showing the reorganization of the TC between Oct. 11 and Oct. 13. Finally, the full suite of functional ORB features is shown as a function of time (bottom), with the original time series (*gray*) smoothed by an exponential weighted moving average (EWMA, *black*) with decay chosen to achieve a roughness (average value of $|d^2 f(t)/dt^2|$) of $0.15\sigma/\text{hr}^2$ across the basin.

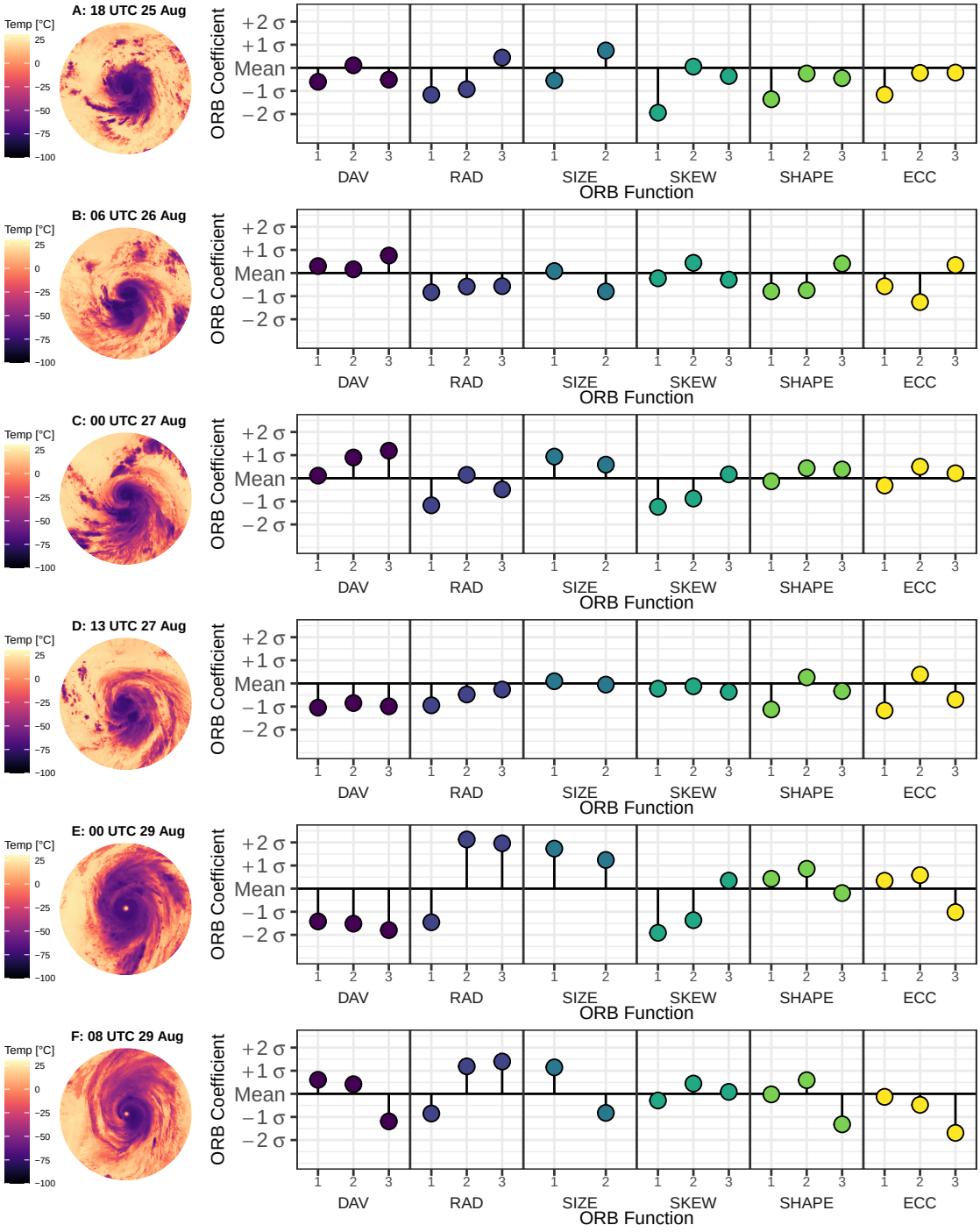


Figure 3: *Functional ORB features for selected stamps:* Infrared imagery (left) and scaled functional ORB features (right) for Hurricane Katrina [2005] at times A-F. Note that functional ORB features are given as number of sample standard deviations from the sample mean value. The low DAV values and high RAD1/RAD2 values at point E mark the clearest organization and Eye-eyewall structure.

## Other Model Results

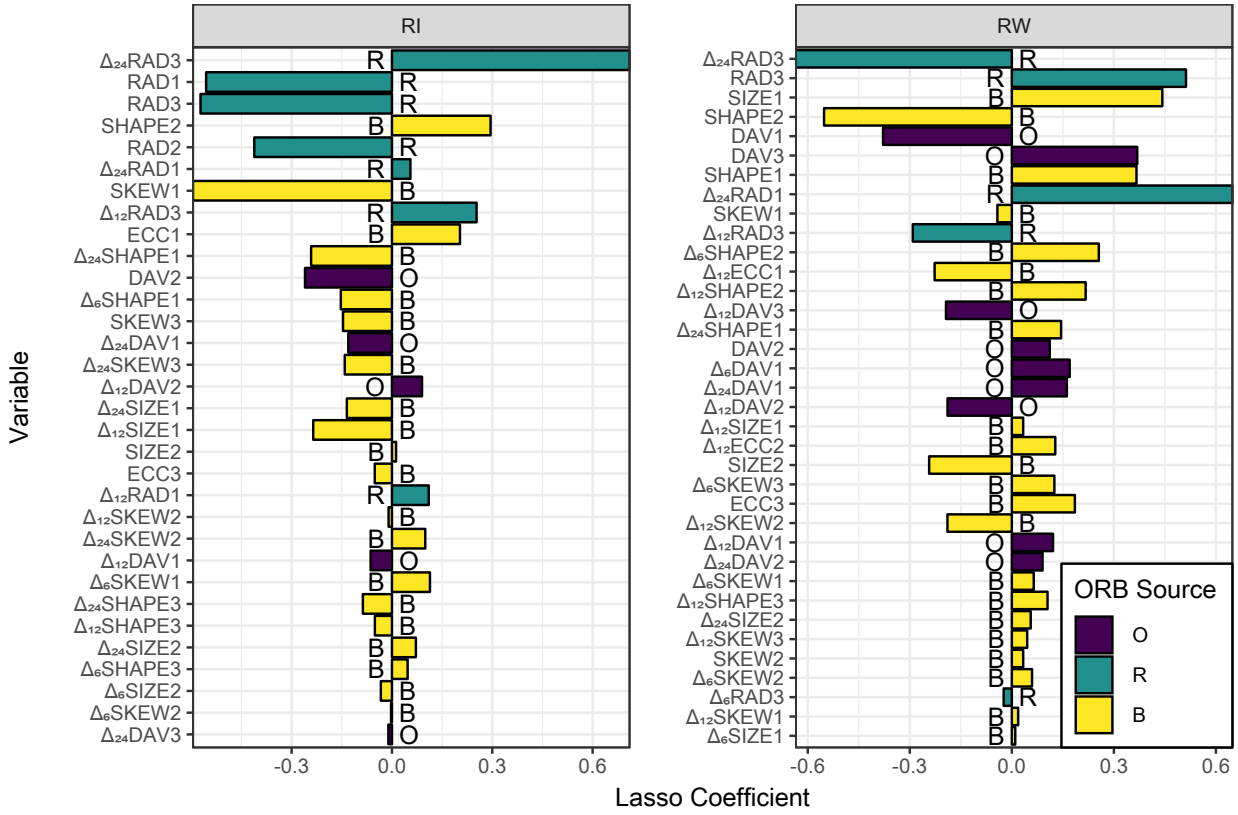


Figure 4: *Logistic lasso with* `ORB`*-Only predictor set; NAL:* Coefficients in logistic lasso for rapid change in the NAL under the `ORB`-Only predictor set. Radial structure and the bulk asymmetry measures (`SHAPE` and `SKEW`) dominate the RI classifier, while overall $\text{CTT}_b$ (`SIZE1`) and `DAV` measures also appear in the RW classifier.

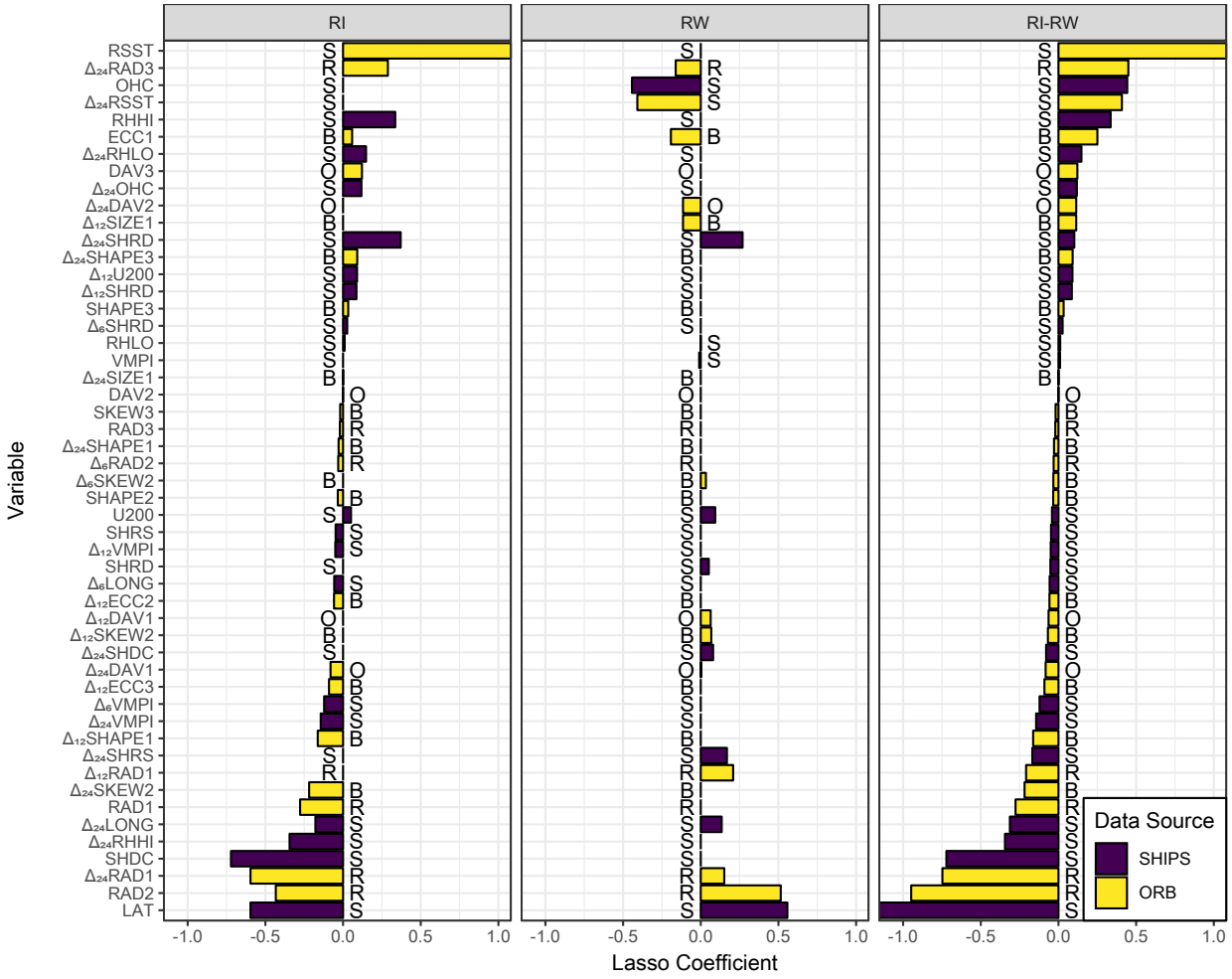


Figure 5: *Logistic lasso with SHIPS + `ORB` predictor set; ENP:* Coefficients in logistic lasso for rapid change in the ENP under the SHIPS + `ORB` predictor set. The presence of `RSST` (Reynolds sea surface temperature) in the RI classifier and `OHC` (ocean heat content) in the RW classifier provides an example of arbitrary selection between correlated predictors.

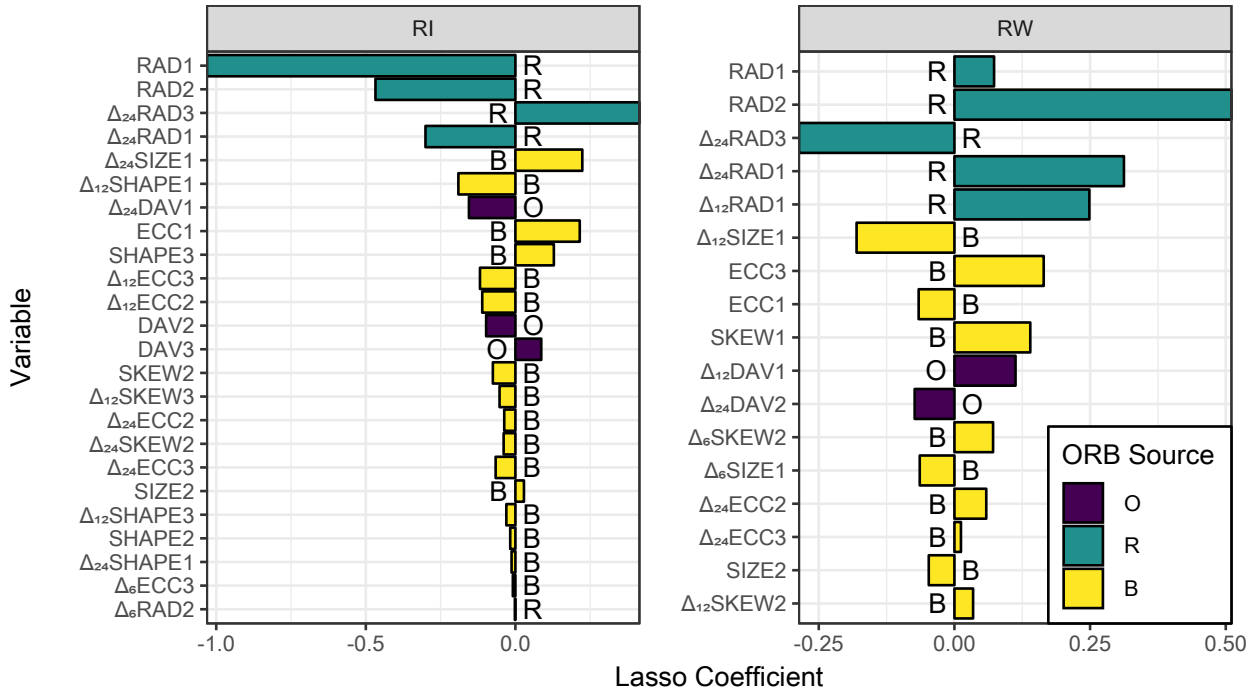


Figure 6: *Logistic lasso with `ORB`-Only predictor set; ENP:* Coefficients in logistic lasso for rapid change in the ENP under the `ORB`-Only predictor set. Radial structure still dominates the `ORB`-Only classifiers. Both classifiers are greatly simplified when compared to their NAL counterparts (Figure 4).

## Predictor Importances

The classifier performance tends to be consistent across the three methods: lasso, random forest (RF) and Xgboost (XGB). Likewise, the variables deemed important are relatively consistent between models. We demonstrate this below by plotting the relative importance for the combined top-5 variables in each method for 2 different basin–event-type–predictor-set combinations.

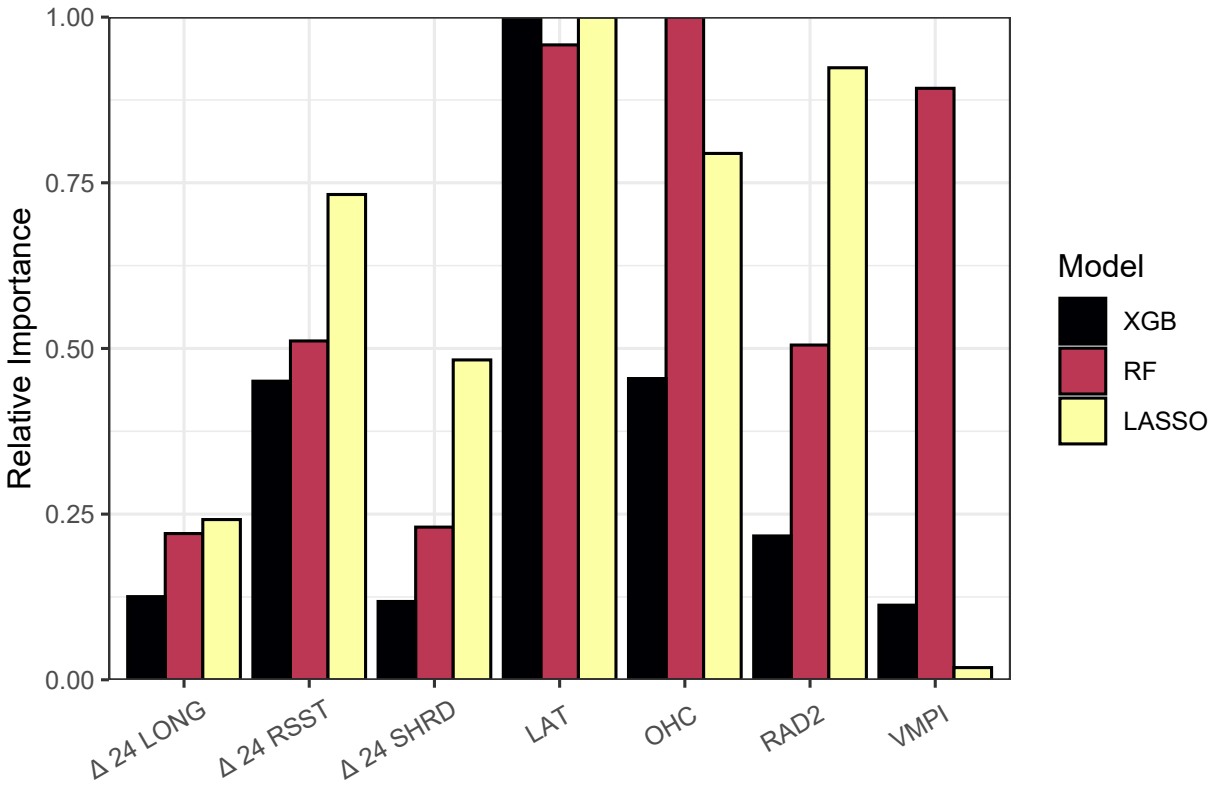


Figure 7: *Variable Selection for RW in the ENP using SHIPS+ORB:* The bars represent the importance of selected variables in each classification method normalized to a maximum of 1. The variables included were top-5 in at least 1 model; `VMPI` was important only in the RF model while $\delta_{24}$`LONG` was narrowly top-5 in the XGB model only.

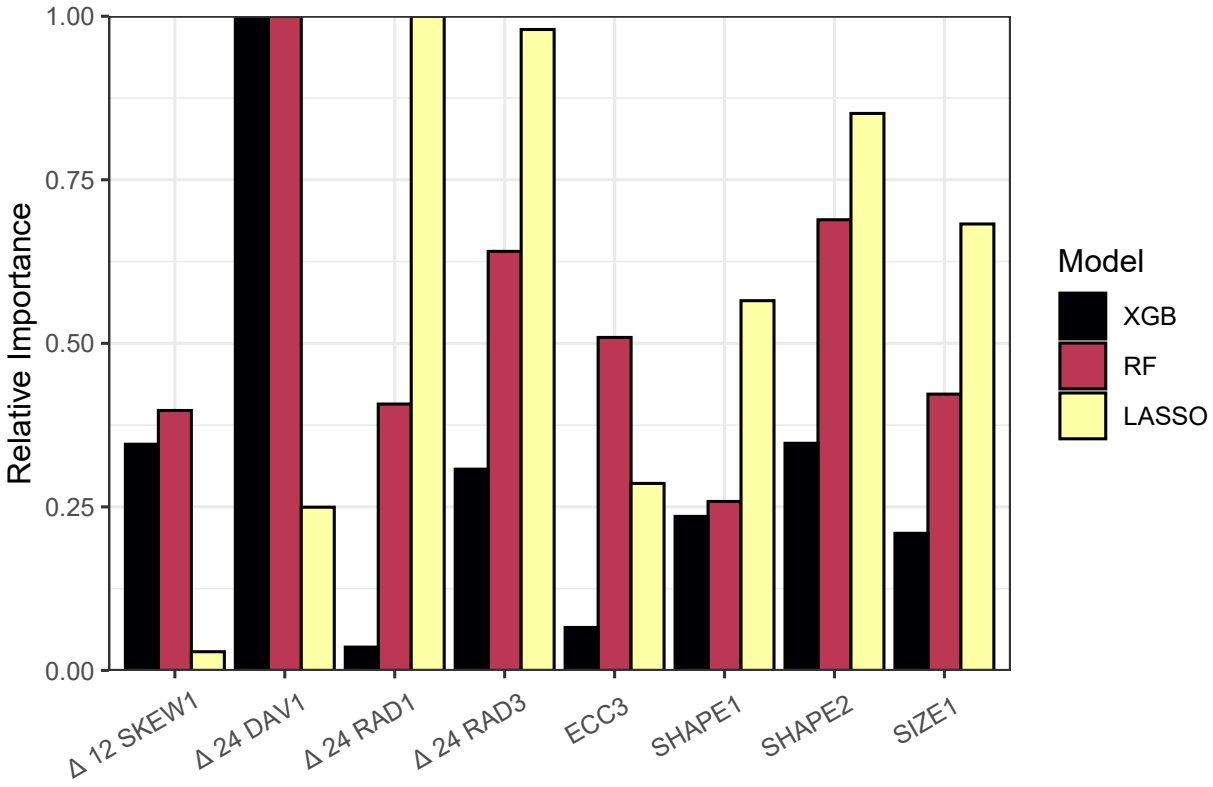


Figure 8: *Variable Selection for RW in the NAL using* `ORB`*-only:* The bars represent the importance of selected variables in each classification method normalized to a maximum of 1. The variables included were top-5 in at least 1 model; RF and lasso again agree in ranking reasonably well, but XGB and RF much more heavily weight the 24-hour change in `DAV1` than does the lasso.